

## Rotor Dynamics without Equations

F. C. Nelson

Professor of Mechanical Engineering  
Tufts University  
Medford, MA 02155 USA  
Frederick.nelson@tufts.edu



**Dr. Frederick Nelson** is Professor of Mechanical Engineering at Tufts University in Medford, Massachusetts, USA. He is a member of the Board of Directors of the Vibration Institute and a fellow of the American Society of Mechanical Engineers, Acoustical Society of America, and the American Association for the Advancement of Science. He has been a Visiting Professor at the Institute for Sound and Vibration Research and the Institut National des Sciences Appliquées de Lyon.

### ABSTRACT

The analysis of the lateral and torsional motion of spinning rotors is replete with applications of Newton's and Euler's equations. Sometimes the intricacies of these equations overshadow their simpler physical meaning. This paper attempts to compensate for this by explaining the dynamic behavior of spinning rotors without writing any equations.

### 1. INTRODUCTION

The first successful rotor model was proposed by Föppl in 1895. It consisted of a single disk centrally located on a circular shaft, without damping. It demonstrated that supercritical operation was stable. Unfortunately, Föppl published his work in a German civil engineering journal, which was little read, if at all, by the rotordynamics community of his day.

In 1919 Jeffcott conceived the same model, this time with damping, and published his work in a widely read English journal. As a result, in the UK and the USA a single disk rotor is called a Jeffcott rotor. Over time many variations of the Jeffcott rotor have been studied but its most frequent features are a single, rigid disk mounted on a circular, flexible shaft, which is supported by bearings at each end. This is the configuration that will be assumed in this paper, see Figure 1.

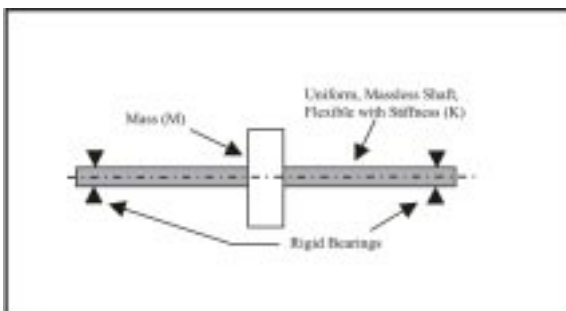


Figure 1: The Jeffcott Rotor, Courtesy of [1].

The Jeffcott rotor model is obviously an oversimplification of real-world rotors but it nevertheless assists an understanding of many features of real-world rotor behavior, including critical speeds, gyroscopic action, and the destabilizing effect of internal damping. The full richness of the model is demonstrated in the book by Krämer [2].

### 2. NATURAL WHIRLING (PRECESSIONAL) FREQUENCIES AND MODES

The dynamics of a rotor are not exactly the same as the dynamics of a spring-mass system. The reference state of the latter is stationary while that of the former is rotational. Nevertheless, they share the existence of natural frequencies and natural mode shapes. Let the rotor have a spin speed of  $\Omega$  rad/s ( $60\Omega/2\pi$  rpm) and let  $\Omega$  be such that the rotor's reference state is stable. Then if an impact is applied in the same sense as  $\Omega$ , the rotor will whirl in a bent shape around its reference state at a rate of  $\omega$  rad/s ( $\omega/2\pi$  Hz). This is called Forward Whirling (FW). If the impact is opposite to the sense of  $\Omega$ , the rotor will undergo Backward Whirling (BW). The frequencies of these whirling motions are called *natural whirling (precessional) frequencies* and the associated shapes are called *natural whirling (precessional) modes*.

For a Jeffcott rotor with a non-central disk the FW and BW natural whirling frequencies are different functions of  $\Omega$  and will diverge when plotted against  $\Omega$ . The root-

cause of this divergence is the wobbling of the non-central disk during whirling. The interaction of this wobbling motion with the disk angular momentum vector produces an effect that increases the FW frequency and decreases the BW frequency. Although somewhat of a misnomer, this effect has acquired the adjective: *gyroscopic*. This gyroscopic effect is particularly prominent if the disk polar mass moment of inertia is much larger than that of the shaft.

The determination of the natural whirling frequencies and modes is a mathematical eigenvalue problem; that is, a problem in linear algebra and not a problem in vibration response. As in all eigenvalue problems the eigenvectors (natural whirling modes) are *indefinite*, being determined only to a multiplicative constant. Choosing a value for this constant is known as normalization. There are numerous eigenvalue solvers that one can employ but, of course, one should never accept the results of a solver without performing a reality check. For example, the fundamental FW and BW eigenvalues (natural whirling frequencies) can be checked by means of the Rayleigh method described by Lalanne and Ferraris in [3].

### 3. OPERATIONAL DEFLECTION SHAPES

Consider a Jeffcott rotor as in Figure 1 that has an unbalanced disk, i.e. a disk with an offset  $e$  between its center of mass (point G) and its center of rotation (point S) as in Figure 2.

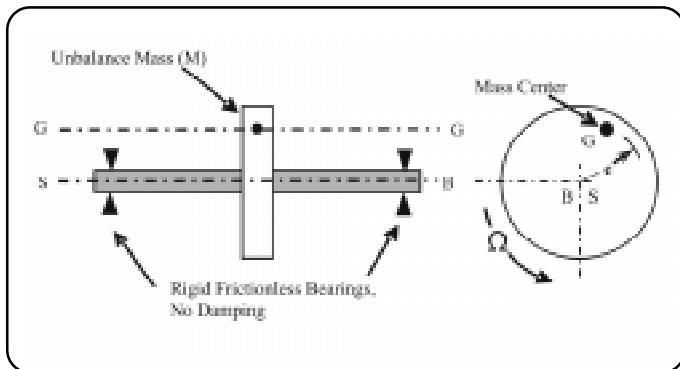


Figure 2: Jeffcott Rotor Configuration for Low Spin Speed, Courtesy of [1].

As the rotor spin speed increases, this offset will cause point S to move outward relative to the bearing centerline (axis B) thereby producing a forced whirling motion. Forced whirling is a dynamic response motion with a *definite shape*, called the *Operating Deflection Shape* (ODS); a typical example is shown in Figure 3. It is important that the natural whirling modes not be confused with the ODS. Although different in concept, they are related. For each spin speed a set of weighting factors can be found such that the weighted sum of the normalized natural whirling

modes is equal to the ODS. This is known as the rotordynamic *expansion theorem*

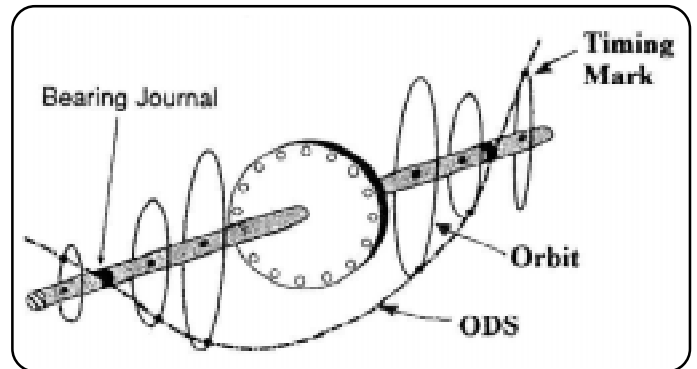


Figure 3: A Typical Operating Deflection Shape (ODS) for Jeffcott Rotor, Courtesy of [1].

In this review we shall be concerned mainly with an ODS for which the whirling rate is equal to the spin speed, a condition known as *synchronous whirling*.

Synchronous whirling is caused by unbalance (imbalance) and plots as a straight line of positive slope in  $\omega, \Omega$  coordinates. It is also referred to as the one-times-spin speed line and labeled 1X.

### 4. EQUATIONS OF MOTION

To make the major point of this brief discussion of the rotordynamic equations of motion (EOM), it is sufficient to limit the model to a low spin speed, synchronous, undamped Jeffcott rotor. The point is the avoidance of a conceptual trap, which must be avoided if one is to be true to the principles of mechanics.

There are two basic ways to formulate the EOM: write them with respect to stator-fixed (inertial) coordinates (XYZ) or write them with respect to rotor-fixed (non-inertial) coordinates (xyz). Rotor-fixed coordinates are best if the rotor geometry is non-axially symmetric and stator-fixed coordinates are best if the bearing and/or seal force distributions are non-axially symmetric.

In stator-fixed coordinates, the centripetal (center-seeking) acceleration of the disk center of mass (cm) is caused by radial forces at the bearings, see Figure 4(a). In rotor-fixed coordinates, the cm is motionless but since the coordinate system is non-inertial the cm acquires a centrifugal (center-fleeing) force, which is reacted by radial forces at the bearings, see Figure 4(b). In stator-fixed coordinates, the rotor forcing function (the right-hand-side of the EOM) is generated by geometric effects, not force effects.

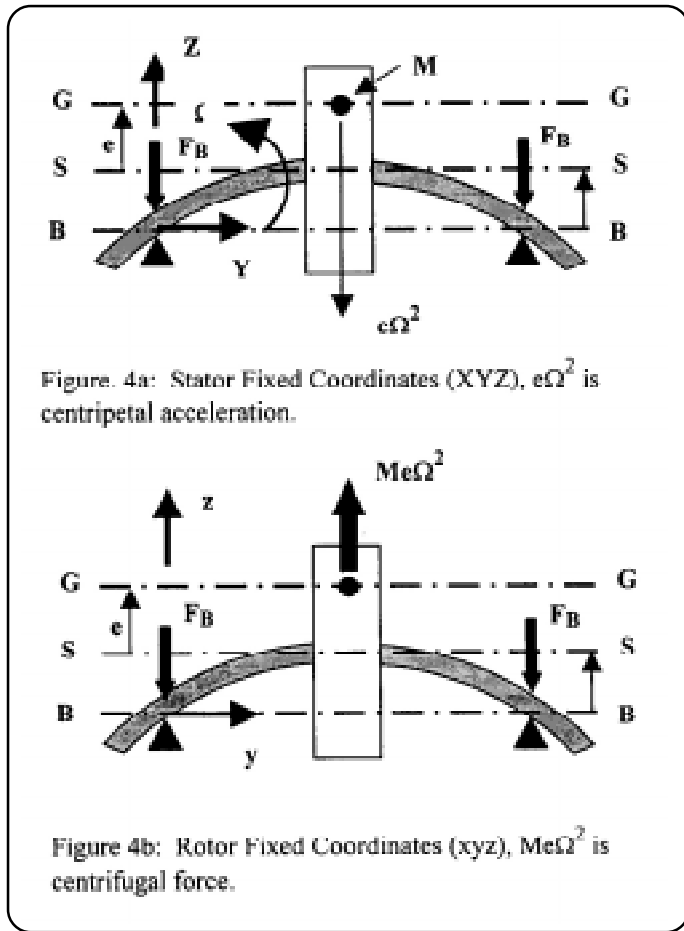


Figure 4: Undamped, Low Spin Speed Jeffcott Rotor in Stator and Rotor Fixed Coordinate Systems, Adapted from [1].

The conceptual trap is the use of centrifugal force in stator-fixed coordinates. The principles of mechanics tell us that centrifugal force does not exist in inertial coordinates. But the gods of mechanics must like irony, because if you fall into this trap you are still likely to get the correct EOM.

The EOM for non-synchronous whirling and for non-central disks can be found in Krämer's book (plenty of equations there!).

**5. LATERAL CRITICAL SPEEDS**

In 1924 Wilfred Campbell had the useful idea of superimposing the synchronous response line on the FW and BW natural whirling frequency lines, giving us the Campbell diagram (interference diagram). At this point, we change our model to a Jeffcott rotor with its disk at the one-third point of its shaft and with the geometry and material properties given in Figure 5; its resulting Campbell diagram is shown in Figure 6. The intersections of the synchronous line with the FW and BW natural frequency curves are denoted by points A and B and the corresponding spin speeds by  $\Omega_A$  and  $\Omega_B$ . These intersections represent a matching of

forcing due to unbalance and natural frequencies and, as such, are a rotating system's analog to resonance in a stationary system. Resonance is associated with a local peak in amplitude (o-p) and a shift in phase. The same is true for a rotating system only with the substitution of the term critical speed for resonance.

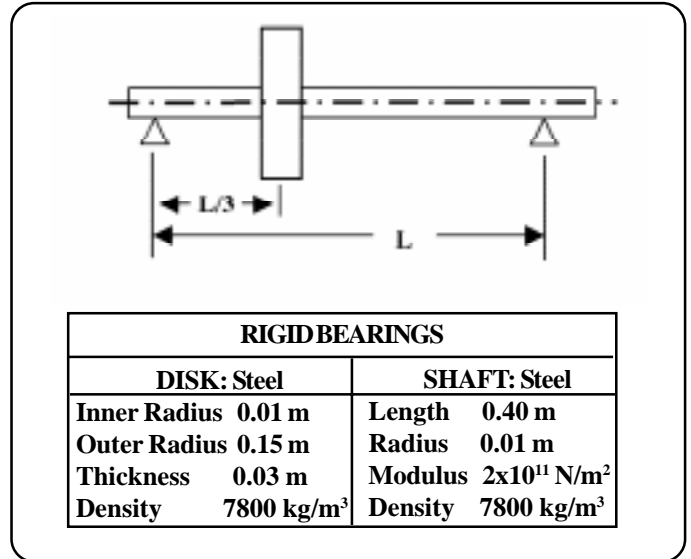


Figure 5: Material Properties and Dimensions of a Jeffcott Rotor, Courtesy of [3].

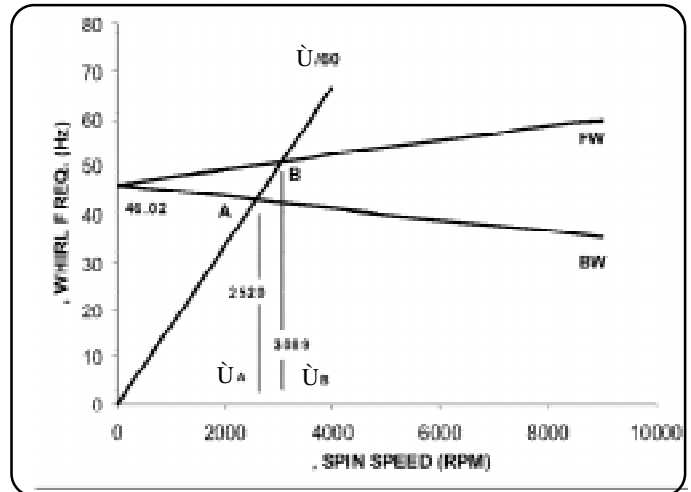


Figure 6: Campbell Diagram of the Rotor in Figure 5, Courtesy of [3].

The rotor of Figures 5 and 6 is a special case since it can be shown that  $\Omega_B$  is a critical speed but  $\Omega_A$  is not. That is, at  $\Omega_A$  the steady state unbalance response curve shows no peak and no phase shift. This is illustrated in Figure 7. The reason for this unusual behavior is the axial symmetry of this single-disk rotor. One can show that the BW mode vector is orthogonal to the unbalance force vector and, as such, energy cannot be fed into the backward whirl. If the rotor is not axially symmetric (asymmetric), these vectors are no longer orthogonal and both  $\Omega_A$  and  $\Omega_B$  become critical speeds. Since real world rotors have various asymmetries this would be the usual case. Nevertheless, it

is certainly curious that a FW force can excite a BW motion.

Figure 8 shows the undamped, steady state, unbalance response of the rotor in Figure 5 with an asymmetry along the Z-axis (a single spring at the two-thirds point of the shaft) and, in contrast to Figure 7, it shows response peaks at both  $\Omega_A$  and  $\Omega_B$ .

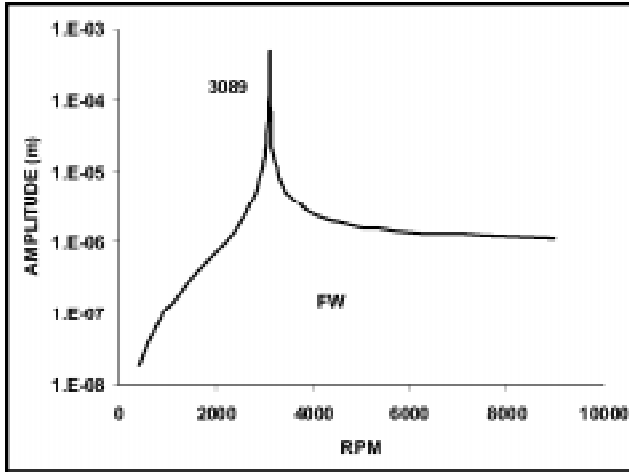


Figure 7: Mass Unbalance Response of an Axially Symmetric Rotor Corresponding to Figure 5, Courtesy of [3].

Figure 8 has another feature that deserves discussion. The response curve is a plot of the maximum amplitude at some point on the rotor's ODS. In accordance with the rotordynamic expansion theorem, this ODS is a weighted sum of the forward and backward natural whirling modes, in this case producing the elliptical orbits shown at the bottom of the Figure. More interestingly, the weighting factors are a function of spin speed so that for  $\Omega < 2520$  rpm the FW mode is dominant and the ODS is in FW. Above 2520 rpm the BW mode becomes dominant and the ODS is in BW. The rotor then passes through the BW critical speed at 2642 rpm. This whirl conversion occurs again at 2888 rpm, the ODS converting back to FW. The FW critical speed is passed at 3377 rpm and the ODS remains in FW for all higher spin speeds. This behavior is mirrored in the changing orbits at the bottom of the Figure. Notice that the elliptical orbits flatten into straight lines at the FW-to-BW and BW-to-FW transition points. Flat orbits also occur in rotors with mixed whirl where they separate the regions of FW and BW.

In practice, the BW response peaks are not usually observed. FW synchronous circular orbits have “frozen stresses”, i.e. the stresses do not cycle. On the other hand, BW synchronous circular orbits have stresses that cycle at a frequency of  $2\Omega$ . Hence if rotor damping is stress cycle dependent, BW modes can have much higher damping than FW modes and, furthermore, this damping increases with  $\Omega$ . This higher damping can suppress the BW response peaks below the level of API (American Petroleum Institute) code

recognition or even visual observation.

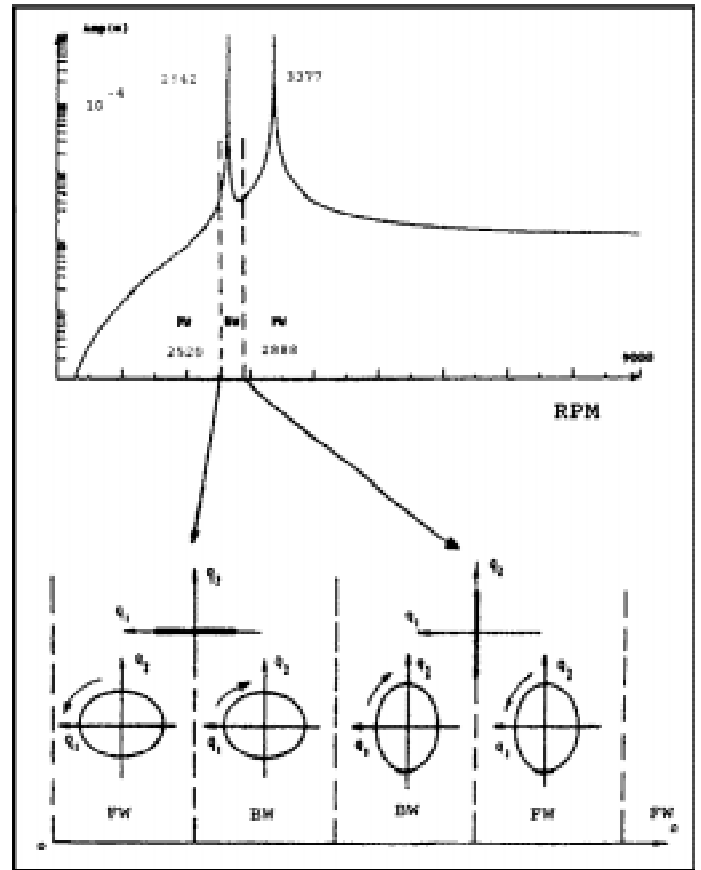


Figure 8: Mass Unbalance Response and Orbits of an Asymmetric Rotor Corresponding to Figure 5, Courtesy of [3].

Up to this point only rigid bearings have been considered. The flexibility of oil-filled journal bearings is usually incorporated into rotordynamics using a linear approximation, i.e. in the form of two direct and two cross coupled stiffnesses for small motions around the steady load position of the shaft. Similarly, four damping coefficients can be determined. These eight dynamic coefficients are functions of spin speed, among other parameters. Bearings with finite stiffness will affect a rotor's natural whirling frequencies and thereby its critical speeds. See Figure 9, which is an example of a critical speed map (CSM). Notice that when the bearings are soft, i.e. much less stiff than the shaft, the two lowest critical speeds are “rigid” body modes, one cylindrical (translational) and the other conical (pivotal). As the bearings increase in stiffness, these “rigid” modes are transformed into bending (flexural) modes. To insure adequate damping from the bearings it is advisable to keep the ratio of the combined bearing stiffness to the shaft stiffness below a value of about 7.

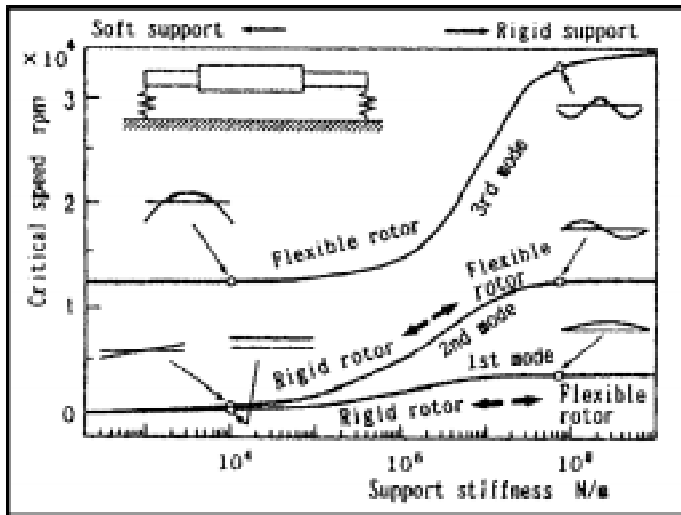


Figure 9: A Typical Critical Speed Map (CSM), Courtesy of [4].

The CSM provides a convenient format for determining how the speed dependent bearing stiffnesses affect critical speeds. For example, consider a bearing with different direct vertical stiffness,  $k_{zz}$ , and direct horizontal stiffness,  $k_{xx}$ . When the spin speed dependence of these coefficients are overlaid on a CSM, the intersections indicate the resulting flexible shaft-flexible bearing critical speeds, see Figure 10. Notice that there are, in fact, two critical speeds at each crossing point. These are called split criticals. Rotors have been known to reverse their whirl direction between *split criticals*. In the cases where split criticals are well spaced, one should avoid concluding that the first two criticals have been passed when only the first split criticals have been passed. The CSM is also useful in deciding whether the intended operating speed range is compatible with the locations of the lateral critical speeds.

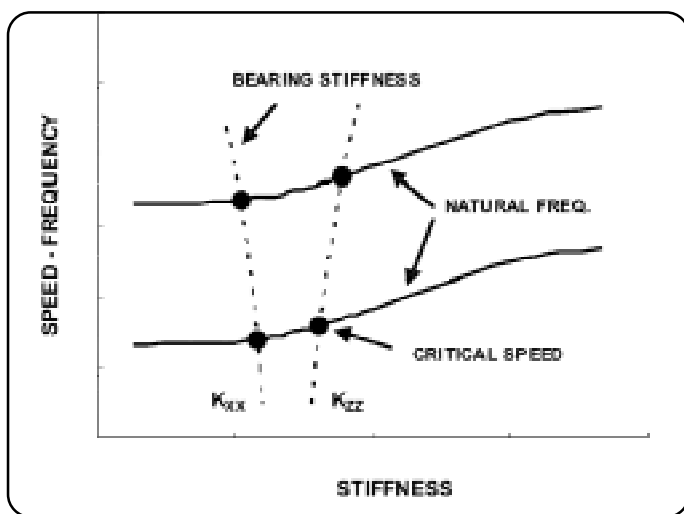


Figure 10: CSM with Superimposed Spin Speed Dependent Bearing Stiffness, Courtesy of [5].

The effect of the external damping in the bearings on lateral critical speeds was studied by Jørgen Lund in one

of the landmark papers of rotordynamics [6]. Lund solved the damped rotor eigenvalue problem and thereby revealed several new phenomena. Among them the fact that for sufficiently high damping up to two modes can become overdamped and thus disappear from the Campbell diagram, along with their critical speeds. Subsequently, Lalanne and Ferraris verified this and, in addition, found that it is possible for highly damped FW and BW loci to cross thereby inverting the order in which one would expect to encounter their critical speeds. However, the major benefit of Lund's analysis is the ability to obtain the damped (complex) eigenvalues. The real parts of these complex eigenvalues provide a mode-by-mode measure of the margin against instability. For this reason, some API codes require the calculation of the damped eigenvalues.

If the rotor has prestress, additional stiffness terms enter the EOM and affect the critical speeds. Such effects are important in rotors with high thrust loads. In the case of thin shell-like rotors additional stiffness terms may be required to account for so-called spin stiffening. If the prestress is due to a steady torque, the critical speeds will be reduced although this effect is small and commonly ignored unless the torque-induced stress is very large. However, the superposition of a pulsating torque on the steady torque can initiate lateral instability and, as such, it is the more important torque effect.

Of course, flexible bearings are housed in flexible support structures, which usually have strongly asymmetric stiffness properties. Only rarely do these flexible support structures have no effect on critical speeds. In fact, as Eshleman [5] has pointed out, if there is no effect, the support structure is probably oversized.

If the rotor is part of a prototype or a commissioned machine, the critical speeds can be obtained by measurement. There are many general purpose and specialized signal analysers that, together with appropriate proximity probes, can measure the 1X amplitude and phase as a function of spin speed. These data can then be used to generate a *Bode diagram* and/or a *Nyquist diagram*. A peak in the Bode amplitude diagram corresponds to a critical speed provided it is also associated with a phase change. If the Bode diagram has an amplitude peak without a phase change, it is likely to be a support structure resonance. In practice, these data are usually obtained from a coast-down test of the machine from an initial state of thermal equilibrium. An alternate display of such data is a *spectrum cascade diagram*. However, cascade diagrams do not contain phase information.

When the rotor spin speed approaches one of the critical speeds the rotor ODS approaches the corresponding

natural whirling mode shape. By running near a critical speed and making amplitude measurements at discrete axial locations, one can use interpolation to estimate the natural whirling mode shape. However, such measurements must be regarded with care since more than one mode shape can fit the same set of discrete data.

## 6. TORSIONAL CRITICAL SPEEDS

The effect of torsional vibration on a rotor is sometimes slighted, often to the eventual chagrin of the designer since it is a frequent failure mode for rotating machinery. Paradoxically, only a few rotordynamics textbooks discuss torsional vibration and even then somewhat briefly, Walker's text [7] being an important exception.

The general principles for finding torsional critical speeds are similar to those for lateral critical speeds. However, there are some specific differences. The torsional natural frequencies are independent of spin speed so they plot as horizontal lines on the Campbell diagram. Also, the primary source of 1X excitation is shaft eccentricity rather than unbalance. In addition, torsional damping is different. It is usually much less than lateral damping, which makes the avoidance of torsional critical speeds all the more essential for machine reliability and durability. The torsional damping in journal bearings and rolling element bearings is usually assumed to be zero. The major sources of external torsional damping are the characteristics of the rotor's load and/or its driver. Internal damping arises from the hysteretic damping of the rotor material (usually small) and/or the drive train couplings (usually large). Information on torsional damping is rare but some can be found in [8].

The determination of the appropriate excitation lines on a Campbell diagram is a central issue in torsional vibration analysis. A typical diagram is shown in Figure 11, taken from [8].

It represents just the motor-shaft section of a pump driven by a motor through a gearbox. The motor is a two-pole induction motor with a variable frequency six pulse VSI (voltage source inverters) drive. Its operating speed range is 1000 rpm to 1800 rpm. The motor shaft gear has 25 teeth. The excitation lines will then have the following order numbers: motor 1X, 2X, variable frequency drive 6X, 12X, 18X (higher orders are not shown), gear mesh 25X.

An eigenvalue analysis showed that the first four natural frequencies are 50 Hz, 220 Hz, 340 Hz, and 500 Hz. These are shown as horizontal lines on Figure 11. Inspection of the resulting intersections, shown as black circles on this figure, indicates that there are six putative critical speeds of

the motor shaft in its operating speed range, none of which are on the 1X line. Analysis of the pinion, pump shaft, and impeller system in [8] reveals another four critical speeds, one of which is on the 1X line. Due to low levels of the excitation or high levels of damping, some of these critical speeds may be ignored. The ones that cannot be ignored become the design-sensitive critical speeds. It is good practice to verify this by performing a forced vibration analysis.

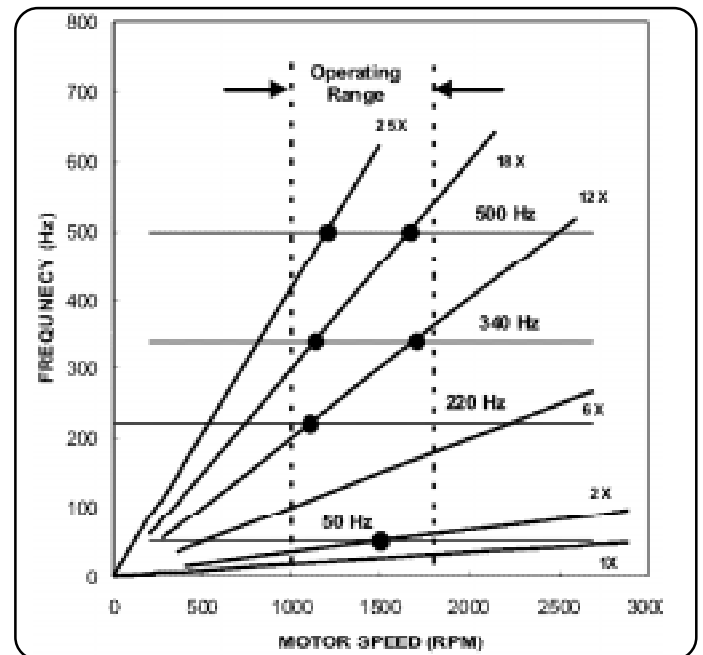


Figure 11: Torsional Campbell Diagram for the Motor-Shaft Section of a Pump Driven through a Gearbox, Courtesy of [8].

Everything above is for steady state vibration. In the case of electrical turbomachinery trains, transient vibration can govern the design. Reference [7] considers a turbomachinery train that has five steam turbines, a generator, and an alternator, all in tandem. The system is subjected to a full-load rejection, i.e. the turbines abruptly stop delivering driving torque and the generator and alternator rotors simultaneously stop generating electrical power. A transient analysis shows that the peak transient torque in the alternator shaft is 7 times its steady state value. The moral of this example is that some shaft spans may have to be designed to carry much more torque than is predicted by the steady state analysis.

As for lateral critical speeds, torsional critical speeds can be obtained by measurement. However, the measurement of the oscillating twist of a rotor is complicated by the fact that the rotor is spinning. As stated in [9]: “Lateral vibration is easy to measure and difficult to predict. Torsional vibration is difficult to measure and easy to predict”

## 7. INSTABILITY

Passive torsional systems do not become unstable. On the other hand, lateral instabilities have long vexed the rotordynamics community. No sooner had Jeffcott demonstrated that supercritical operation of an externally damped rotor was stable than Newkirk described a supercritical instability due to internal damping (1924) and a year later, an instability due to oil action in journal bearings. Subsequently, additional instabilities have been discovered.

If a linear, stationary rotor has symmetric, positive definite mass, stiffness, and damping matrices, it will be stable, i.e. all perturbations will decay back to the reference state. However, the addition of rotor spin gives a rotational bias to the rotor and, as a result, these matrix symmetries are broken. In particular, the mass, stiffness, and damping matrices can acquire a skew-symmetric component. *Indeed, the peculiarity of rotordynamics is the occurrence of such skew-symmetric matrices alongside the familiar symmetric ones.* It can be argued that these skew-symmetric components are zero or inconsequential for the mass and external damping matrices; however, the skew-symmetric component of the stiffness matrix is consequential.

Analysis shows that the symmetric component of the stiffness matrix produces conservative restoring forces and its elements are properly called stiffnesses. The skew-symmetric component produces non-conservative tangential forces that can insert power into the rotor during each revolution and hence it can be destabilizing. It is clearly inappropriate to call the skew-symmetric matrix a stiffness matrix; instead, it is conventional to call it the *circulatory matrix* to reflect its circulatory action.

Two common rotordynamic phenomena give rise to a circulatory matrix: internal damping within the rotor and fluid stiffness cross coupling in the rotor's bearings and seals. In the former, the elements of the circulatory matrix are the equivalent internal viscous damping coefficients; in the latter, they are the fluid cross coupling stiffness coefficients.

Internal damping is due primarily to friction at rotor component interfaces. When the power inserted by internal damping exceeds the power extracted by external damping (e.g. support bearing damping and windage damping), the rotor will become unstable. For this instability to manifest itself the rotor must be operating above a critical speed whose mode shape promotes interfacial friction and it must be in FW. The end state of this instability is FW subsynchronous whirling at a critical speed. Much practical progress has been made in eliminating or reducing the sources of internal damping in modern built-up rotors to the

point where today this instability is seldom encountered.

Fluid stiffness cross coupling occurs in many bearings and some seals. The forces associated with cross coupling stiffness can insert power into the rotor and if this power exceeds the power extracted by the direct fluid damping forces, the rotor will become unstable. The spin speed at which this instability threshold occurs is best determined by solving the damped eigenvalue problem. The spin speed at which the real part of the damped (complex) eigenvalue first passes through zero from negative values is the instability threshold. Mitigating the effects of cross coupling in bearings or seals is something of an art form, dealing with tradeoffs among bearing clearance, bearing loading, and bearing asymmetry, as well as many other parameters. Bearing clearance has a particularly tricky tradeoff: increasing bearing clearance reduces the cross coupling stiffnesses but it also reduces the external damping, making internal damping more of an instability threat. The somewhat paradoxical rule is: loose is better than tight but not too loose. The most common means of mediation is the use of tilting-pad bearings, which have little, if any, cross coupling stiffness. The uninitiated, or the uncertain, in this art form would do well to consult the work described in [10] and [11].

The usual end state of fluid-induced instability in a rotor supported by oil-filled journal bearings is *oil whirl*, although it is possible for the end state to skip oil whirl and appear as *oil whip*. Figure 12 shows a spectrum cascade diagram of oil whirl and oil whip.

Several features of this diagram are worth noting:

1. The instability threshold is subcritical (although it is possible that the threshold is supercritical with respect to an overdamped mode).
2. Oil whirl is a harbinger of oil whip.
3. Oil whirl and oil whip are subsynchronous.
4. The frequency of oil whirl tracks the spin speed at a fixed ratio slightly less than 0.5 (0.475 in the case shown).
5. The frequency of oil whip is constant and near a flexural critical speed, typically the lowest one.
6. The rotor excursions during oil whirl and oil whip exceed those due to unbalance and can cause the journal eccentricity ratio to approach unity.
7. Due to nonlinear oil action at high journal eccentricity, the motions associated with oil whirl and oil whip are bounded, nonlinear cycles known as *limit cycles*.

8. The size of the oil whip limit cycle is larger than that of oil whirl.

The rotor shape during oil whirl is predominately rigid body hence its behavior is governed by bearing properties; the rotor shape during oil whip is predominately flexural with nodes at or near the bearings hence its behavior is governed by rotor properties. Thus, as shown, oil whirl is speed dependent and oil whip is speed independent.

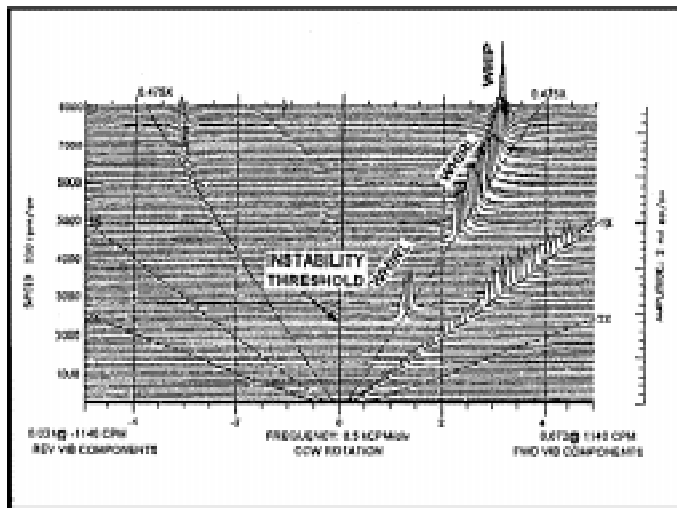


Figure 12: Cascade Plot showing Oil Whirl and Oil Whip in a Bench Top Rotor Rig. Courtesy of [4].

Oil whirl and oil whip motions are superimposed on the synchronous motion giving rise to orbits with an internal loop. They are FW motions, although Figure 12 shows evidence of a small amount of BW motion, which may be due to a small rub.

Oil whirl is the most common fluid-induced instability end state in real-world machines and oil whip is the most dangerous. Real-world machines have been allowed to run with oil whirl provided the whirl limit cycle does not use up more than 50% of the bearing clearance. However, it should be remembered that subsynchronous motion will generate alternating stresses and a fatigue failure of a high energy rotor is a highly hazardous event.

Finally, in assessing rotor instability as a whole, it is useful to repeat some advice offered in [12]: “Instabilities...pose a serious challenge to the designer, since there are many different mechanisms to be dealt with. The difference between a stable and an unstable machine may be very small in magnitude and subtle in nature, so that the occurrence will vary from unit to unit of the same design and even from time to time on the same unit”

Given the modeling uncertainties that affect the prediction of instability thresholds and our imperfect understanding of the physics of many of them, it is not

surprising that the best predictor is full-load, full-speed factory testing.

## 9. CLOSURE

The premise of this review paper has been that physical insight into rotordynamic phenomena is every bit as useful as an understanding of the associated EOM and their computational algorithms. In this respect, the author has been motivated by a comment by Childs in [13]: “...the quality of [rotordynamic] predictions...has more to do with the physical insight of the rotordynamicist than the particular algorithm used...superior algorithms ...will not cure bad models or a lack of engineering judgment”

## 10. ACKNOWLEDGEMENT

The author would like to thank Mr. H. E. Alpaugh for his considerable help in editing and formatting the text and for several refinements of the figures.

## 11. REFERENCES

1. Eisenmann, R.C. and Eisenmann, R.C. Jr., Machinery Malfunction, Diagnosis, and Correction, Prentice Hall, 1998
2. Krämer, E., Dynamics of Rotors and Foundations, Springer-Verlag, 1993
3. Lalanne, M. and Ferraris, G., Rotordynamics Prediction in Engineering, 2nd Edition, Wiley, 1997
4. Yamamoto, T. and Ishida, Y., Linear and Nonlinear Rotordynamics, Wiley, 2001
5. Eshleman, R., “Resonance and Critical Speed Testing: Part III, Critical Speed Testing Techniques, Vibrations, vol. 7, no. 1, 1991
6. Lund, J., “Stability and Damped Critical Speeds of a Flexible Rotor” ASME Journal for Industry, vol. 96, no. 2, pp 509-517, 1974
7. Walker, D., Torsional Vibration of Turbomachinery, McGraw-Hill, 2004
8. Corbo, M. and Malanoski, S. “Practical Design Against Torsional Vibration” 21st Annual Meeting of the Vibration Institute, 1997
9. Leader, M. and Kelm, R., “Practical Implementation of Torsional Analysis and Field Measurement” National Technical Training Symposium of the Vibration Institute, 2004

- 10.** Leader, M., "Rotor Dynamics as a Tool for Solving Vibration Problems" National Technical Training Symposium of the Vibration Institute, 2003
  - 11.** Leader, M., A Short Course on Journal Bearings, Applied Machinery Dynamics, P.O. Box 157, Dickerson TX, 1998
  - 12.** Ehrich, F. and Childs, D., "Self-excited Vibration in High-Performance Turbomachinery" Mechanical Engineering, pp 66-79, May 1984
  - 13.** Childs, D., Turbomachinery Rotordynamics, Wiley, 1993
-